Coral Reefs
https://doi.org/10.1007/s00338-025-02696-9

RESEARCH

Structure and complexity of a rariphotic coral ecosystem in the Gulf of Aqaba (Red Sea)

Giovanni Chimienti[1] · Fabio Marchese[2] · Sam J. Purkis[3,4] · Viktor Nunes Peinemann[2,5] · Lucía Pombo-Ayora[2,5] · Marta Ezeta Watts[2,5] · Tullia I. Terraneo[2] · Michael L. Berumen[2,5] · Ameer A. Eweida[3,6] · Mattie Rodrigue[7] · Francesca Benzoni[2,5]

Received: 4 February 2025 / Accepted: 16 June 2025

Abstract A series of explorations along the Saudi Arabian coast of the Gulf of Aqaba (Neom territory, Red Sea) led us to discover and characterize a Rariphotic Coral Ecosystem (RCE) spanning a depth range of 110–200 m. The primary architects of this ecosystem are the azooxanthellate scleractinian corals *Madracis interjecta, Dendrophyllia minuscula*, and *Rhizopsammia compacta*. These corals build the framework of three different bioherms (i.e., *M. interjecta* mound-like bioherms, *D. minuscula* shelf-like formations, and *R. compacta* bio-stalactites), encrusted, cemented and reinforced by a suite of benthic taxa including other scleractinian corals, bryozoans, foraminifers, molluscs, and serpulids. The RCE is characterized by a rich associated community of antipatharians and alcyonaceans, and it provides habitat for numerous fish taxa. Light-dependent zooxanthellate scleractinians and macroalgae, present in the lower mesophotic coral ecosystems at shallower depths (80–102 m) at the same sites, were absent in the examined RCE. North of the city of Magna, the RCE develops to its fullest complexity, with a combination of all three bioherms arising at multiple levels from the vertical reef wall, giving the appearance of a structured "coral palace." Due to its unique structure, complexity, and richness, the RCE here described—and the Magna site in particular—represent a priority for conservation framed by amplified urgency related to the ongoing coastal development in Saudi Arabia.

Keywords Azooxanthellate corals · Marine animal forest · Mesophotic coral ecosystem · Neom · Saudi Arabia

Introduction

Mesophotic coral ecosystems (MCEs) are conventionally defined as coral-dominated communities occurring from the limit of presence of photophilous algae down to the depth limit for sunlight penetration to sustain photosynthesis (Lesser et al. 2009). MCEs are mostly built by light-dependent scleractinian corals at tropical latitudes (Kahng et al. 2010; Turner et al. 2017). At temperate latitudes, by contrast, they are primarily constructed by azooxanthellate corals and crustose coralline algae (Turner et al. 2019; Chimienti et al. 2020), with a rich, non-photosynthetic community (e.g.,

Supplementary Information The online version contains supplementary material available at https://doi.org/10.1007/s00338-025-02696-9.

✉ Giovanni Chimienti
giovanni.chimienti@uniba.it

✉ Francesca Benzoni
francesca.benzoni@kaust.edu.sa

[1] Department of Biosciences, Biotechnology and Environment, University of Bari Aldo Moro and CoNISMa LRU, Bari, Italy

[2] Red Sea Research Center, Biological and Environmental Science and Engineering (BESE) Division, King Abdullah University of Science and Technology (KAUST), Thuwal, Saudi Arabia

[3] Department of Marine Geosciences, Rosenstiel School of Marine, Atmospheric, and Earth Science, University of Miami, Miami, FL, USA

[4] Khaled Bin Sultan Living Oceans Foundation, Annapolis, MD, USA

[5] Marine Science Program, Biological and Environmental Science and Engineering Division, King Abdullah University of Science and Technology (KAUST), Thuwal, Saudi Arabia

[6] Saudi Red Sea Authority, Jeddah, Saudi Arabia

[7] OceanX, New York, NY, USA

Published online: 01 July 2025

azooxanthellate scleractinians, alcyonaceans, antipatharians, sponges). Recent explorations have highlighted the presence of a faunal break immediately below the mesophotic zone and above the deep aphotic regions—the rariphotic zone (Baldwin et al. 2018; Stefanoudis et al. 2019). More than a simple transitional zone, the rariphotic hosts specific marine communities adapted to live in an environment with perceptibly illumination, albeit insufficient to support photosynthesis. This threshold, historically set at 1% of the surface photosynthetically active radiation (Lesser et al. 2009), is currently considered coinciding with 1% of downwelling irradiance at 490 nm (surface blue light sensu Marra et al. 2014). The overall maximum depth of mesophotic investigations at 90–110 m (Loya et al. 2019) has led to a general overlooking of coral ecosystems in the lower boundary of the mesophotic zone and in the rariphotic zone, just above the known coral ecosystems in the aphotic deep sea (Roberts et al. 2009). Under conditions particularly amenable to coral growth, mesophotic and rariphotic ecosystems are able to produce an elaborate carbonate architecture and often include the so-called marine animal forests (sensu Rossi et al. 2017). Here, the structural complexity is delivered by ecosystem engineers that convey multiple ecological functions, including the provision of feeding, nursery, and spawning grounds for many associated species (Blyth-Skyrme et al. 2013; Rosa et al. 2016; Loya et al. 2019; Chimienti 2020). Due to multiple anthropogenic threats spanning unsustainable fishing pressure to pollution, these ecosystems are considered vulnerable based on the life-history traits of their primary ecosystem engineers, such as corals, and their protection is a priority worldwide (FAO 2009).

Evolution of the Red Sea marine fauna has been shaped by geographic isolation, latitudinal gradients, and high salinity and temperature, even at depth (Roder et al. 2013; Berumen et al. 2019; Manasrah et al. 2019). The absence of perennial exorheic riverine input into the hyperarid Red Sea delivers exceptional water clarity, with the mesophotic zone locally extending as deep as 156 m in the Gulf of Aqaba (Eyal et al. 2019b). That semi-enclosed gulf, a northern extension of the Red Sea, hosts such a diversity of ecosystems that it likely represents a distinct biogeographic zone, at least for shallow water coral communities (Sheppard and Sheppard 1991; Eyal et al. 2019b; Purkis et al. 2022a; Terraneo et al. 2023). Deep-sea areas of the Red Sea have been explored since the end of the nineteenth century through pioneering expeditions, such as the Austro-Hungarian Pola Expedition in 1895–1898 and the John Murray Expedition in 1933–1934 (Marenzeller 1907; Gardiner and Waugh 1939; Scheer and Pillai 1983) and, more recently, using Remotely Operated Vehicles (ROVs) and submersibles (Roder et al. 2013; Qurban et al. 2014; Purkis et al. 2022b; Nolan et al. 2024), while its lower mesophotic and rariphotic waters remained relatively unexplored for a few more decades. In fact, the first reports of Red Sea mesophotic and rariphotic ecosystems came from submersible dives conducted in the 1980s at various locations offshore Israel, Egypt, Djibouti, and Sudan (Fricke 1982, 1996; Fricke and Hottinger 1983; Fricke and Knauer 1986). In the Gulf of Aqaba, Fricke and colleagues discovered coral-dominated benthic assemblages growing over biogenic formations between 100 and 200 m depth, mainly on a flat to gently sloping seafloor, interpreted at the time to represent drowned Pleistocene reef terraces. Bioherms built by the azooxanthellate colonial scleractinian *Madracis interjecta* (Fricke and Hottinger 1983: Fig. 4), a Red Sea endemic, were observed together with *Dendrophyllia* cf *minuscula* at a smaller scale (Fricke and Hottinger 1983: Fig. 3). Those authors also reported other associated azooxanthellate scleractinians, mainly Dendrophylliidae, Caryophylliidae and Flabellidae. A considerable body of literature has been published on the ecology and physiology of upper mesophotic corals in the Gulf of Aqaba focusing on adaptations of light-dependent zooxanthellate scleractinians (Eyal et al. 2019a, b; Tamir et al. 2019). However, coral ecosystems in the lower photic zone and their bioconstructional potential have remained insufficiently characterized in the area.

Since 2020, three scientific expeditions facilitated by OceanX along the Saudi Arabia coast of the Gulf of Aqaba have provided the opportunity to explore a wide bathymetric range (from 50 to 1770 m depth) using ROV and submersibles. Acoustic seabed mapping, video surveys, benthic invertebrate reference collections, and water column characterization were systematically performed. This allowed an unprecedented wealth of information to describe and characterize in detail the Gulf of Aqaba (GoA) Rariphotic Coral Ecosystem (RCE), highlighting its unique structure and composition in comparison with the lower MCEs in the same area. Notably, a combination of edaphic and oceanographic conditions north of Magna (Neom territory, southeast Gulf of Aqaba) supported the establishment and development of the richest and most complex GoA RCE site found to date. Based on these findings, here we provide a detailed description of a RCE occurring between 100 and 200 m depth—straddling the lower limit of the mesophotic zone and the rariphotic zone—whose complexity was only partially known thus far. We provide a characterization of the GoA RCE north of Magna, highlighting how this discovery poses an urgent call for management and conservation considering the region's rapid coastal development.

Materials and methods

Visual surveys and sampling

The coastline along the Saudi Arabia Gulf of Aqaba was explored during three oceanographic cruises aboard

M/V OceanXplorer: the Deep Blue Expedition in October–November 2020, the Relationship Cultivation Expedition in June 2022, and the Neom Gulf of Aqaba Expedition in October 2023 (Fig. 1a–c). Site choice was driven by bathymetry and seabed morphology. A total of seven ROV and four submersible dives were carried out along the depth profile at the southeast coastline of the Gulf of Aqaba (Fig. 1c–d; Table 1).

Visual surveys were carried out using an Argus Mariner XL108 ROV (*Chimaera*) and two Triton 3300/3 submarines (*Nadir* and *Neptune*). The ROV was equipped with a Kongsberg HiPaP 501 Ultra Short Base Line (USBL) acoustic tracking systems, and a complex light-cameras apparatus with one DSPL Super wide-angle CCD camera for landscape view and one HDTV 1080p F/Z color camera for detailed observations. Each submersible was equipped with a Sonardyne Ranger Pro2 USBL system and several light and camera systems, including a Wide Angle Red DSMC2 Helium 8 k Canon CN-E15.5–47 mm lens and a macro Red DSMC2 Helium 8 k Nikon ED 70–180 mm F4.5–5.6D. Submersibles and ROV featured a10 cm laser scale for size and area measurements, a conductivity-temperature-depth (CTD) probe (RBR Maestro CTD), and a Schilling T4 hydraulic manipulator for sampling.

In 2020 and 2022, transects were run perpendicular to the coastline from 235 up to 50–100 m depth, depending on the transect (Table 1). ROV and submersible cruised at 1–3 m from the seafloor to film both benthic and benthopelagic species. Each ROV and submersible transect had a duration of 2–9 and 2–3 h, respectively, depending on the substrate and the number of samples collected. Ad hoc sampling of small portions of substrate and benthic taxa was performed with the manipulator arm from both assets, allowing a reference collection for the main coral taxa. Sampled material was tagged, subsampled for further genetic and morphological identification, and curated onboard the vessel. Once ashore, the material was analyzed at the King Abdullah University of Science and Technology (KAUST, Saudi Arabia) where it is currently stored. Geological samples were air-dried and preserved at KAUST and at the University of Miami (Florida, USA). Identification of the laminar micrite crusts was based on images and description by Brachert and Dullo (1991) from the same basin. On the 2023 expedition, to further assess the structure and species composition of the Magna RCE, ROV transects were run parallel to the coastline at three sites in the lower mesophotic between 80 and 103 m and between 118 and 128 m depth, corresponding to the depths of the lower MCE and of the observed RCE.

Seafloor mapping

High-resolution bathymetry data were collected during expeditions in 2020 and 2023 using high-resolution multibeam echosounder system (MBES) mounted on surface and underwater platforms. In 2020, a bathymetric survey of the Saudi Arabian side of the Gulf of Aqaba were conducted aboard the M/V OceanXplorer during the Deep Blue Expedition. A Kongsberg EM712 MK2 (70–100 kHz) was used to survey the area, covering depths ranging from 100 to 1770 m (Purkis et al. 2022a, b; Nolan et al. 2024). In 2023, high-resolution nearshore bathymetry (10–400 m depth) was collected using a Metalshark 38 boat (the M\V OceanXplorer 12 m support vessel) equipped with a dual-head Kongsberg EM2040C (200–400 kHz). Fine-scale bathymetry at the Gulf of Aqaba RCE site was further refined using the ROV Chimaera equipped with a Teledyne Reason T50-P (190–420 kHz). Sound velocity profiles (SVP) to calibrate MBES data were obtained using Expendable Bathy-Thermograph (XBT) and Sea-Bird 911 CTD systems. SVP profiles were processed with Sound Speed Manager v2023.0.10 (Masetti et al. 2017).

Bathymetric data were processed using QPS Qimera v2.6.2 workflow, resulting in three bathymetric models at different resolutions: (a) a 30 m resolution model covering the Saudi Arabian Gulf of Aqaba from the 2020 Deep Blue Expedition, (b) a 5 m resolution model from the OceanX Metalshark nearshore data, and (c) a 1 m resolution model derived from the ROV Chimaera dataset from the 2023 Neom Gulf of Aqaba Expedition, (Fig. 1c–e).

Water column characterization

In 2020, water column profiles (depth, temperature and salinity parameters) were obtained using a Sea-Bird 911CTD during two casts performed from the M/V OceanXplorer (Fig. 1c, f). Moreover, an RBR CTD was mounted on the ROV to record the same profiles during each ROV dives. In 2022 and 2023 expeditions, the RBR CTD was deployed on every ROV dive, providing continuous environmental profiling (Fig. S1). Both CTDs were calibrated prior to the cruise. The SBE's Seasoft software and RBR Ruskin software were used for data extraction, and Origin Pro 2022b (v9.9.5) and ODV (v5.6.7) were used for processing and visualization of the CTD data.

A total of ten casts were performed to characterize temperature, salinity, and chlorophyll-a (chl-a) in the study area: two Sea-Bird (CTD24 and 25; Fig. 1f) and six RBR dives (CHR0043, CHR0044, CHR0045, CHR0392, CHR0393, and CHR0394; Fig. S1) during the end of summer and the beginning of the transitional season (October–November 2020 and 2023), and two RBR dives (CHR0311, NTN0181; Fig. S1) during early summer (June–July 2022). Chl-a was also used to detect a defined deep chlorophyll maximum (DCM) sensu Lohrenzen (1966).

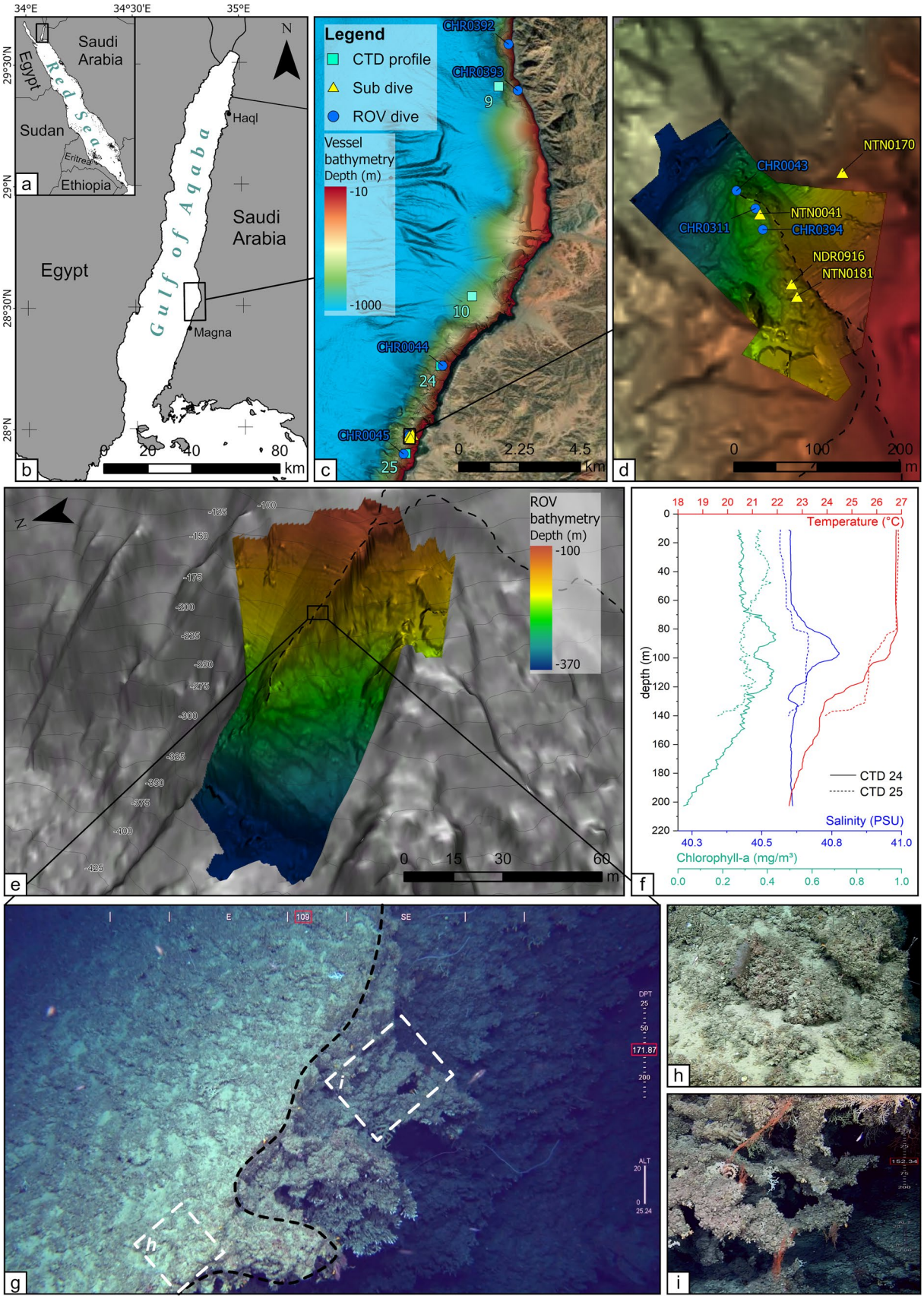
34°E
34°30'E
35°E
29°30'N
29°N
28°30'N
28°N
N
Saudi Arabia
Egypt
Red Sea
Sudan
Eritrea
Ethiopia
Haql
Gulf of Aqaba
Saudi Arabia
Egypt
Magna
a
b
0 20 40 80 km
Legend
CTD profile
Sub dive
ROV dive
Vessel bathymetry
Depth (m)
-10
-1000
CHR0392
CHR0393
9
10
CHR0044
24
CHR0045
25
c
0 2.25 4.5 km
NTN0170
CHR0043
NTN0041
CHR0311
CHR0394
NDR0916
NTN0181
d
0 100 200 m
e
ROV bathymetry
Depth (m)
-100
-370
0 15 30 60 m
Temperature (°C)
depth (m)
CTD 24
CTD 25
Salinity (PSU)
Chlorophyll-a (mg/m³)
f
g
h
i

◂**Fig. 1** Geographic, geomorphological, and water column settings of the Rariphotic Coral Ecosystem (RCE) described in this study. **a**, **b** Geographic setting of the survey area within the Red Sea and Gulf of Aqaba regions. **c** Position of ROV dives (blue dots), submersible dives (yellow triangles), and Sea-Bird CTD casts (cyan squares) in the area. Two bathymetric models are shown: the M/V OceanXplorer (30 m resolution) for deeper areas and the Metal Shark boat (5 m resolution) for the coastal zone. **d** Magnification of the richest RCE area found, showing ROV and submersible dives overlaid on the ROV 1-m high-resolution bathymetric model. Dashed lines indicate the mass-wasting scars creating the vertical/overhanging wall where the RCE is located. **e** 3D-oriented model of the ROV bathymetry showing the morphology of the mass-wasting scar and along the depth gradient. The model is re-oriented to mirror the orientation of video footage in g. **f** Sea-Bird CTD profiles collected during the 2020 Deep Blue Expedition. **g** Example of the inclination break at the upper boundary of the RCE with **h** detail of hard substrate patches above the break and **i** detail of the RCE bioherms below it

Video analysis

In total, 31 h of video were collected (13 h in 2020, 9 in 2022 and 9 in 2023). Videos were processed and visualized using Adobe Premiere Pro software v25 to synchronize timestamps with navigation and environmental data, review and trim video segments of interest, and extract still frames for subsequent annotation and analysis. The presence/absence of the GoA RCE was noted in each video, from its deepest to its shallowest occurrence. Within this bathymetric range, changes in substrate inclination, species composition, main scleractinian ecosystem engineer, and type of bioherm were directly annotated using the software. For qualitative and occurrence assessment purposes, still images were extracted from the ROV videos to document the presence and depth of bioherms, benthic organisms and fish of the GoA RCE. This documentation occurred when these features were first visible during a dive and the still image provided a clear view suitable for recording them. For benthic organisms, image-based taxonomic identification was possible through comparison with the in vivo morphology of the collected identified specimens. Methodological details for the taxonomic identification based on samples and photographs are provided as supplementary materials.

For a quantitative assessment and comparison of the lower MCE and GoA RCE benthic assemblages' composition, image stills were obtained from ROV videos of dives CHR0311 (RCE depth range 143–166 m), CHR0392 (lower MCE depth 89 m; RCE depth 118 m), CHR0393 (lower MCE depth range 80–82 m; RCE depth 119 m), and CHR0394 (lower MCE depth range 102–103 m; RCE depth range 127–128 m). Non-overlapping stills were taken at regular time intervals, excluding: those without laser scale clearly visible; those not perpendicular to the substrate (to avoid potential estimate errors derived from camera lens-substrate image distortion; Pawlik et al. 2022); those depicting less than 1 m^2 or more than 2 m^2 of seafloor (to have enough resolution for benthos identification); with more than 20% of the image represented by black areas. A total of 15 replicates were extracted for the lower mesophotic zone and 20 for the rariphotic zone. For each image still, a photoquadrat was standardized to size using the known 10 cm distance between laser points in the image. Using Coral Point Count with Excel extensions (CPCE; Kohler and Gill 2006), 50 random points were cast on each photoquadrat. A quadrat point-intercept based estimate of percentage cover was obtained for the following biotic and abiotic categories: Zooxanthellate Scleractinia (SZoox); Azooxanthellate Scleractinia (SAzoox); Octocorals except whip-shaped taxa (Octos); Antipatharia except whip-shaped taxa and Zoantharia (Hexa); whip-shaped Antipatharia and Octocorallia (whips); crustose coralline algae (CCA); Bryozoa and benthic Foraminifera aggregation (BryoFor); mobile substrate including sediment and rubble (SR); rocky substrate (RCK). For each photoquadrat, the total proportion for each category was calculated and expressed in percentage. The data was then averaged per category across replicates within each depth zone (expressed as mean ± standard error) to allow a benthic assemblages composition comparison between the lower MCE and the GoA RCE.

Results

Geomorphology and RCE bathymetric zonation

The examined stretch of the Gulf of Aqaba seafloor was characterized by a narrow and variably sloping continental shelf. The euphotic zone hosted light-dependent coral reef communities from the surface to approximately 40 m depth. Below this limit, as light availability further decreased, photosynthetic organisms persisted, but the benthic community composition changed toward more sciaphilous species including mesophotic specialists (e.g., *Leptoseris* cf. *striatus*). There, the role of crustose coralline algae was fundamental, and the abundance and diversity of alcyonaceans and antipatharians increased until 90–110 m depth. Beyond this depth, the seabed continued with variably sized hard substrate patches interspersed with sediment, colonized by a low-density assemblage dominated by alcyonaceans (e.g., *Ellisella* sp.) and antipatharians (e.g., *Allopathes* sp.), with only a minor contribution of scleractinians. Several attempts to sample these hard substrate patches to characterize their composition failed. Therefore, the seafloor nature and the smaller components of the benthic fauna remain unknown. Along this coastal sector of the GoA, located in front of the Dakar deep (1230 m depth), the continental slope lies close to the coastline, and the continental shelf is extremely narrow, ranging from 50 to 200 m wide. The shelf break occurs between 90 and 110 m depth, where the gentle seafloor slope

Table 1 ROV (CHR: *Chimaera*) and submersible (NDR: *Nadir*; NTN: *Neptune*) dives with metadata including start/end coordinates, depth range explored and depth of occurrence of the Rariphotic Coral Ecosystem (RCE) described, as well as temperature (T; °C), salinity (S; PSU) and chlorophyll-a (C; mg/m^3) ranges at the RCE. na: not assessed

Dive	Date	Start latitude	Start longitude	End latitude	End longitude	Depth (m)	RCE depth (m)	RCE T (°C)	RCE S (PSU)	RCE C (mg/m^3)
CHR0043	12/11/2020	28.45757	34.75714	28.45762	34.75712	111–220	114–190	22.7–25.2	40.58–40.81	0.00–0.18
CHR0044	13/11/2020	28.48054	34.76847	28.4793	34.76936	130–230	120–148	23.6–24.8	40.59–40.68	0.06–0.12
CHR0045	13/11/2020	28.45105	34.75549	28.45199	34.75712	120–235	112–129	25–25.5	40.62–40.71	0.12–0.30
CHR0311	24/06/2022	28.45737	34.75737	28.45655	34.75795	117–197	120–197	21.2–22.4	40.49–40.69	0.00–0.24
CHR0392	15/10/2023	28.58812	34.79006	28.58783	34.79080	75–145	117–145	22.8–24.7	40.55–40.64	0.16–0.33
CHR0393	16/10/2023	28.57282	34.79309	28.57238	34.79367	79–120	110–118	23.6–25.1	40.55–40.64	0.28–0.35
CHR0394	17/10/2023	28.45714	34.75745	28.45623	34.75818	102–196	115–187	22.2–25.1	40.38–40.59	0.07–0.31
NDR0916	24/06/2022	28.45656	34.7578	28.45545	34.75912	43–133	98–133	21.7–23.2	40.34–40.65	0.12–0.54
NTN0041	26/10/2020	28.45732	34.75742	28.45552	34.75899	50–200	110–200	na	na	na
NTN0170	24/06/2022	28.45776	34.75844	28.45545	34.75903	42–171	115–171	21.2–22.7	40.40–40.69	0.06–0.24
NTN0181	01/07/2022	28.45642	34.75786	28.45624	34.75916	57–144	108–144	21.3–22.4	40.46–40.68	0.06–0.48

shifts abruptly into a steep, often over-vertical continental slope. Additionally, this sector of the GoA continental margin is characterized by mass-wasting scars (dashed lines in Fig. 1d, e, g) which create a NW–SE oriented slope break, resulting in a vertical wall with a displacement of approximately 40 m featuring overhangs and cavities (Fig. S2a). This entailed a clear shift in light availability for benthic organisms and corresponding faunal composition in favor of assemblages composed of non-light dependent zoobenthos down to more than 200 m depth, including an highly three-dimensional RCE. Small, scattered coralline algae crusts were consistently observed down to 130 m depth. Below the break, cavernous voids extended up to 10 m into the wall and were accessible by submersible allowing bedrock sampling (Fig. S2c, d). Retrieved samples showed the base substrate to constitute bedded siliciclastic sandstone, devoid of fossils, suggesting the substrate to represent elements of the Pleistocene sea-level lowstand coastline. In many cases, this substrate was preserved in its original depositional position. In other cases, rotation of bedding planes and obvious dislocation of blocks indicated common mass-wasting events. Likely during subaerial exposure of the sea-level lowstands, the beds of the siliciclastic deposit were differentially eroded, with some standing proud of the outcrop, interspersed by recessive units. All these processes conspired to deliver a highly rugose vertical to over-vertical seabed. Visually apparent during surveys, the greater the rugosity of the sandstone, the richer the benthic community that developed atop of it. Below 200 m depth, the coral community became simplified and less diverse, with the gradual disappearance of most taxa and an overall reduction in size of the remainder. Laminar micrite crusts became evident (Fig. S2b). Notably, similar crusts were also present from 140 m depth in areas where the rocky wall was covered by sediments and scantly colonized by corals (e.g., when broadly facing north).

Composition of the Gulf of Aqaba rariphotic coral ecosystem

The heterogeneous benthic assemblage identified as the GoA RCE was found at all the explored sites, broadly between 100 and 200 m depth (Fig. 1c–i). The RCE was complex and multispecific, with the calcifying zoobenthos playing a primary role in building and shaping the ecosystem. Colonial azooxanthellate scleractinian corals were the main ecosystem engineers. Among those, *M. interjecta*, *D. minuscula* and *Rhizopsammia compacta* formed the largest colonies and provided substrate and habitat to other benthic organisms. Other common scleractinian species included the solitary Agariciidae *Dactylotrochus cervicornis*, the Flabellidae *Rhizotrochus typus* and *Javania insignis*, the colonial Caryophylliidae *Rhizosmilia valida* and *Cladopsammia*

sp., and other unidentified Dendrophylliidae (Fig. 2a–c). In total, 12 scleractinian taxa were associated to the GoA RCE (Table 2). Other calcifying organisms included foraminifers, bryozoans, serpulids and bivalves. For those, species identification is still uncertain, and the material awaits further studies by specialists. Together, however, they formed an association performing a fundamental functional role in the formation and growth of the RCE bioherms. The remaining ecosystem engineers structuring the GoA RCE were alcyonaceans and antipatharians forming mixed coral forests. Among antipatharians, *Acanthopathes*, *Allopathes*, *Asteriopathes* and *Aphanostichopathes* (Fig. 2d–f) were the dominant genera, together with other unidentified taxa in the families Aphanipathidae, Antipathidae and Myriopathidae.

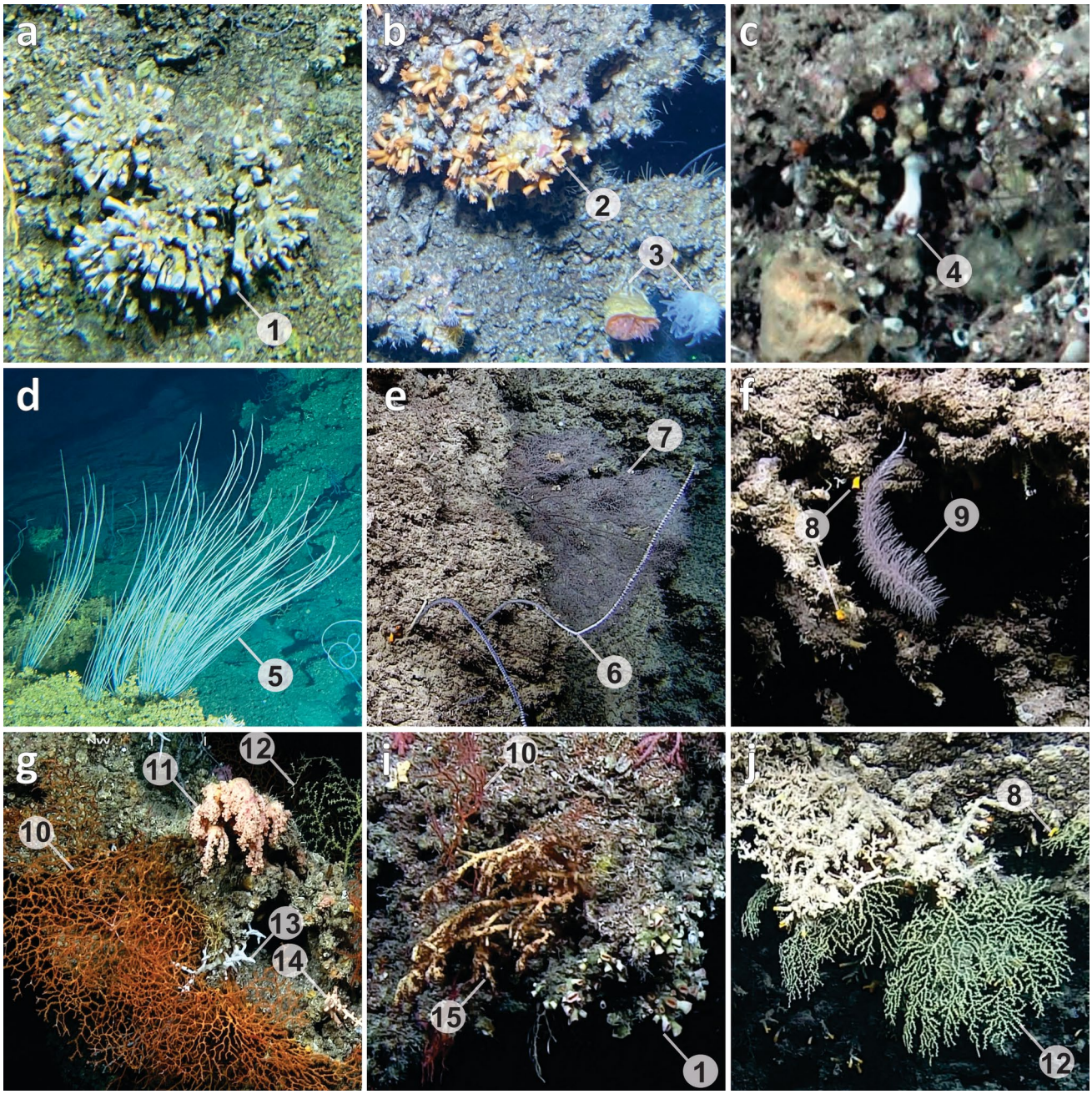

Fig. 2 In situ images of the most commonly observed coral taxa in the Gulf of Aqaba Rariphotic Coral Ecosystem. **a–c** Scleractinia; **d–f** Antipatharia; **g–j** Alcyonacea. Numbers indicate different taxa to the lowest possible identification, such as *Cladopsammia* sp. (1), Dendrophylliidae sp. 2 (2), *Rhizotrochus typus* (3), *Javania insignis* (4), *Allopathes* sp. (5), *Aphanostichopathes* sp. (6), *Acanthopathes* sp. (7), Dendrophylliidae sp. 1 (8), *Asteriopathes* sp. (9), *Melithaea* sp. (10), unidentified Nephtheidae (11), *Acanthogorgia* sp. (12), *Madracis interjecta* (13), *Dendrophyllia minuscula* (14), and *Chironephthya* sp. (15)

Table 2 Anthozoa taxa recorded from the GoA RCE, identified at the lowest possible taxonomic level. Systematics follows the World Register of Marine Species (www.marinespecies.org)

Class	Order	Family	Genus and species
Hexacorallia	Scleractinia	Agariciidae	*Dactylotrochus cervicornis* (Moseley, 1880)
		Caryophylliidae	*Rhizosmilia valida* (Marenzeller 1907)
			Unidentified colonial Caryophylliidae
		Dendrophylliidae	*Cladopsammia* sp.
			Dendrophyllia minuscula (Bourne, 1905)
			Rhizopsammia compacta (Sheppard & Sheppard 1991)
			Unidentified colonial Dendrophyllidae sp. 1
			Unidentified colonial Dendrophyllidae sp. 2
			Unidentified colonial Dendrophyllidae sp. 3
		Flabellidae	*Javania insignis* Duncan, 1876
			Rhizotrochus typus (Milne Edwards & Haime, 1848)
		Pocilloporidae	*Madracis interjecta* Marenzeller 1907
	Antipatharia	Antipathidae	*Allopathes* sp.
			Antipathes sp.
			Stichopathes sp.
		Aphanipathidae	*Acanthopathes* sp.
			Aphanostichopathes sp.
			Asteriopathes sp.
		Myriopathidae	*Myriopathes* sp.
Octocorallia	Malacalcyonacea	Acanthogorgiidae	*Acanthogorgia* sp.
			Calicogorgia sp.
			Muriceides sp.
			Villogorgia sp.
		Astrogorgiidae	*Astrogorgia* sp.
		Euplexauridae	*Euplexaura* sp.
		Melithaeidae	*Melithaea sinaica* (Grasshoff, 2000)
		Nephtheidae	Unidentified Nephtheidae
		Nidaliidae	*Nidalia* sp.
		Siphonogorgiidae	*Chironepthya* sp.
			Siphonogorgia sp.
	Scleralcyonacea	Parisididae	*Parisis* cf *fruticosa* (Verrill, 1864)
		Ellisellidae	*Ellisella* sp.
			Nicella sp.
			Verrucella sp.
			Unidentified Ellisellidae

Forest-forming alcyonaceans were mostly represented by fan-shaped colonies in the genera *Acanthogorgia*, *Chironephthya*, *Euplexaura*, *Melithaea*, *Parisis*, *Astrogorgia* and *Villogorgia* (Fig. 2g–i). Broadly, seven and 16 taxa were observed within antipatharians and alcyonaceans, respectively (Table 2).

Characteristics of the bioherms

The GoA RCE was characterized by three different bioherm typologies, each primarily established by a different foundation species, such as *M. interjecta*, *D. minuscula* and *R. compacta*. Although it was observed at all explored sites, the most structurally complex and diversified GoA RCE was observed along a southwest-facing seafloor north of the city of Magna (Fig. 1b–e). Discovered during 2020 and resurveyed within the following expeditions, the GoA RCE north of Magna is here described in detail. At this specific site, the RCE area extended for 182 m along the seafloor, over a vertical area of 820 m^2, with a structural climax between 120 and 160 m depth.

The *M. interjecta* bioherms were present on flat or gently sloping substrate. Variably developed, reaching up to 2.5 m in diameter and 3.0 m in height, the mound-like bioherms

were covered by other calcifying and non-calcifying organisms at their base, while live *Madracis* fan-like portions were visible at the distal upper end (Fig. 3a–c). Colonies of *M. interjecta* occurred in a broader range of environmental conditions, both shallower and deeper than the depth at which the bioherms were observed. Overall, the *M. interjecta* bioherms represented the less frequently observed bioherm type.

The *D. minuscula* bioherms were uniquely shaped and oriented horizontally, developing from a near vertical hard substrate (Fig. 3d). Spanning from 20 cm to over 2.5 m in length and up to 1 m in width, the framework of these shelf-like formations was primarily built by *D. minuscula* colonies growing perpendicular to the sandstone substrate. In shelves at early stages of development, the foundational dendrophylliid colony was still clearly visible, with the proximal portion of the colony overgrown by benthic foraminifera and bryozoans (Fig. 3e; Fig. S3). As the structure reached a more mature stage, the hard coral skeleton, primed by the encrusting calcifying benthos, was encrusted by other functional groups of calcareous epifauna and overgrown by alcyonaceans and antipatharians, adding to the

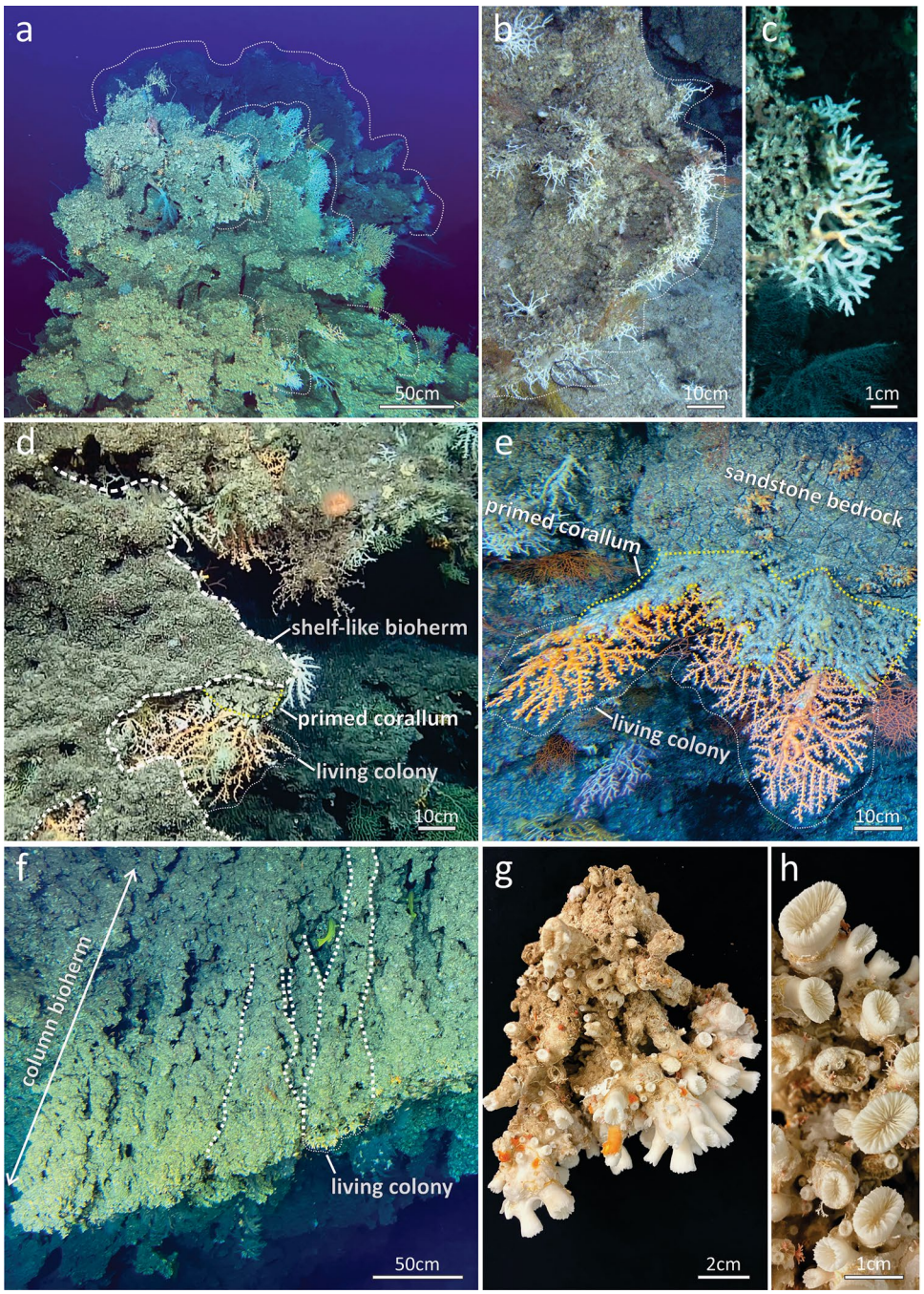

Fig. 3 The different bioherm types and main bioconstructor coral species observed in the Gulf of Aqaba Rariphotic Coral Ecosystem. **a** *Madracis interjecta* bioherm (dotted lines indicate the outer margins of multiple fan-like projections composing the bioherm). **b** Detail of a *M. interjecta* bioherm margin showing the living corals (white) actively forming it. **c** Close-up of a *M. interjecta* colony living on a bioherm. **d** Margin of a shelf-like *Dendrophyllia minuscula* bioherm showing the different stages of the ongoing formation. **e** Single *D. minuscula* colony growing perpendicular to the quasi-vertical sandstone wall. The older and proximal portion of the colony (enclosed by the yellow dotted line) has already been primed by benthic foraminifera and bryozoans overgrowing its skeleton, while the distal portion of it (enclosed by the white dotted line) is still alive, actively growing and typically bright orange in color. **f** Several *Rhizopsammia compacta* biostalactites (dashed white lines show the single stalactites sides) growing together to form a column bioherm typically growing downwards from a cave ceiling, a living (yellow) colony of the coral forming the bioherm by growing downwards is indicated. **g** *R. compacta* specimen and **h** close-up of the corallite morphology

architectural complexity of the final formation. These complex shelves were in turn reinforced by skeletal elements and debris of the epizoic fauna. Developing in proximity to one another, adjacent bioherms fused together into composite shelves. Bivalve molluscs were locally abundant, contributing to the edification and the cementation of the biogenic shelves. Serpulids were ubiquitous, filling small crevices with their calcareous tubes (Fig. S3), while *M. interjecta* was commonly associated with these bioherms as a secondary builder (Fig. 4a–c). Moreover, through a known baffling effect (Rossi et al. 2017), the arborescent alcyonacean and antipatharian colonies enhanced the deposition of smaller grains of sediments falling from the slope above and infilling the porous matrix, nourishing the precipitation of abundant marine-diagenetic cements.

The third bioherm type was composed of *R. compacta* colonies growing downwards from overhangs, forming remarkable formations similar to stalactites, but of biogenic origin (Fig. 3f–h). Like the main bioherms, these bio-stalactites were also cemented and covered by small encrusting epifauna, attaining vertical dimensions up to > 1 m, and > 0.5 m wide. Adjacent bio-stalactites also merged into composite formations. The largest *R. compacta* bioherm was observed hanging down from the overhang created by a mass-wasting event (Fig. 3h). Smaller examples of these formations were also observed growing from the lower side of the *D. minuscula* bioherms, adding to their structural complexity in their final development phase (Fig. 4b, c). Indeed, the pattern of spatial occurrence of the three types of bioherm was driven by both substrate inclination and orientation, leading to their closer association in areas where the seafloor complexity was overall high (Figs. 5 and 6).

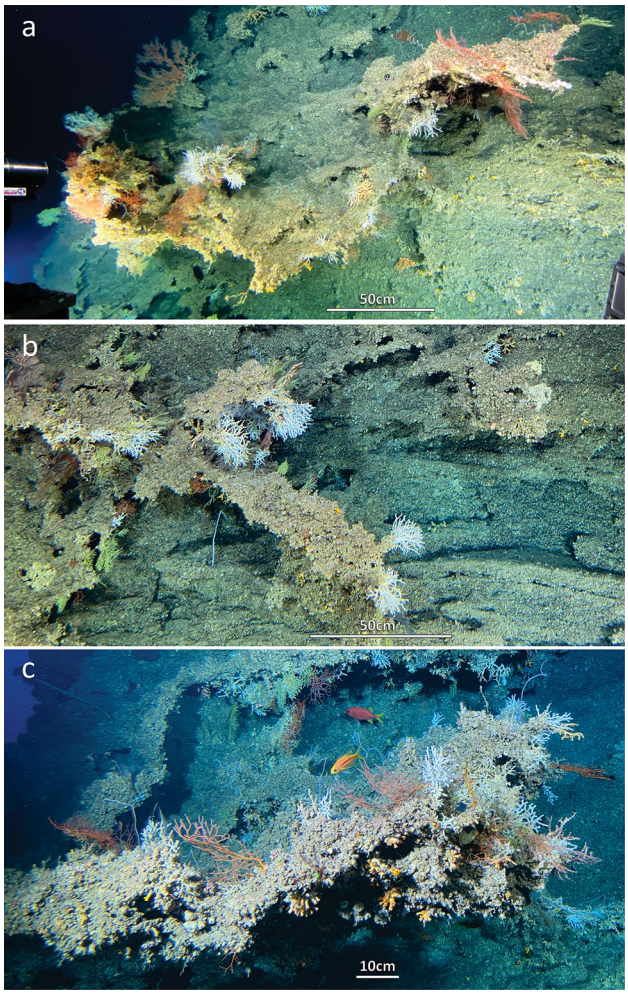

Fig. 4 Structural complexity of the shelf-like bioherms observed along a quasi-vertical wall in the Gulf of Aqaba Rariphotic Coral Ecosystem. **a** shelf-like structures mainly formed by *Dendrophyllia minuscula*, overgrown by scleractinians and alcyonaceans; **b** mixed *D. minuscula* and *Madracis interjecta* bioherms growing outwards from a substrate of bedded sandstone; **c** bioherms and associated benthic assemblage composed of several taxa illustrated in Fig. 2 growing on the top and the bottom part of the shelf-like formation, and associated fish

RCE associated fish fauna

A total of 43 fish taxa belonging to 22 families were recorded during ROV and submersible dives on the GoA RCE, with 35 taxa identified to species level and eight endemics to the Red Sea (Table 3). These observations represent new Red Sea depth records for 15 species and one range extension into the Red Sea (*Seriola rivoliana*).

The fish community of the GoA RCE consisted of a blend of species found on shallow reefs and those exclusive to mesophotic and rariphotic habitats. Among the most abundant and ubiquitous fishes were three species of *Pseudanthias*: *P. gibbosus*, *P. heemstrai*, and *P. taeniatus*. These species formed large, plankton-feeding schools that hovered up to 5 m above the bioherm substrates, particularly in exposed areas with structurally complex substrates. At night, they were observed sheltering in small cavities and crevices of the bioherms to sleep. While individual species tended to dominate specific areas, mixed-species aggregations were also common. Notably, *P. heemstrai* and *P. taeniatus*, previously known to inhabit the upper mesophotic (40–67 m), were observed at greater depths, extending their known habitat range to the lower mesophotic zone. A fourth species, *Pseudanthias* cf. *lunulatus*, was also present. While this may represent a new record for the northern Red Sea and the lower mesophotic zone, the taxonomic identification based on images remains tentative.

Symphysanodon disii frequently formed large, fast-moving schools 1–3 m above the benthos, especially near steep slopes and walls. The species was previously known only from five specimens collected in Aqaba, Jordan and Eilat, Israel (Khalaf and Krupp 2008; Anderson et al. 2011). Our records represent the first in situ recordings of the species

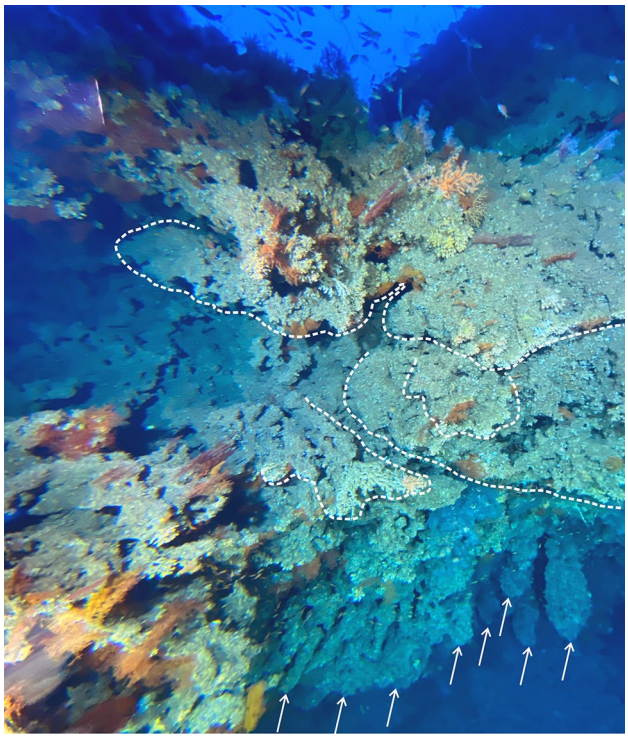

Fig. 5 A general view of the Gulf of Aqaba Rariphotic Coral Ecosystem north of Magna seen from below, showing the highest complexity of mixed bioherms (dotted lines indicate the margins of the shelf-like formations) and *Rhizopsammia compacta* bio-stalactites (white arrows)

and extend its known depth range from 150 to 200 m. Over gently sloping and flat substrates, *Chromis pelloura* was one of the most common species, typically staying just above the benthos.

The three bioherm typologies in the study area provided structurally complex and diverse habitats, supporting a variety of behaviorally cryptic fish species. Larger cavities and overhangs were commonly inhabited by *Myripristis chryseres*, *Sargocentron ittodai*, *Cephalopholis sexmaculata*, and *Epinephelus morrhua*. While most cryptobenthic species are likely to be missed during ROV and submersible dives, at least three distinct species of *Plectranthias* were identified. One of these, identified as *Plectranthias winniensis*, was moderately common in small crevices of the bioherms. Another species, for which high-quality close-up imagery was obtained, likely represents an undescribed species (Luiz Rocha, pers. comm.). This species exhibits long dorsal spines and filamentous caudal fin rays, broadly resembling *Plectranthias ryukyuensis* (Wada et al. 2020).

Several species of elevated conservation concern were observed during the dives. These include single individuals of the pelagic thresher shark (*Alopias pelagicus*), sandbar shark (*Carcharhinus plumbeus*), scalloped hammerhead (*Sphyrna lewini*), and panther electric ray (*Torpedo panthera*), all listed as endangered on the IUCN Red List. Additionally, *Plectropomus marisrubri*, a Red Sea endemic species listed as vulnerable, was recorded. This large predator faces heavy fishing pressure, and our observations provide the first evidence of its utilization of lower mesophotic habitats. While no other recorded fish species are currently listed as threatened, data on many species remain extremely limited, with several species having never been recorded in situ prior to this study.

Hydrographic parameters

During the end of summer and the transitional season, the temperature profiles indicate a well-mixed layer in the upper 80 m, with temperatures nearly stable at ~ 26.5–27 °C. Below 80 m, temperatures decrease progressively with depth, reaching ~ 22–22.5 °C at 200 m. Salinity profiles also exhibit a mixed layer between 20 and 60 m, with values of ~ 40.55–40.65 PSU. Below 60 m, salinity increases, peaking at 95–100 m (~ 40.75–40.8 PSU) before stabilizing at ~ 40.6–40.65 PSU below 100 m.

In early summer, the profiles display slight differences, with a mixed layer extending to 70 m. Within this layer, temperatures are slightly lower (~ 24.5–25.5 °C), and salinity remains relatively uniform (~ 40.45–40.50 PSU) compared to the end of summer. Below 70–80 m, a thermocline is observed, with temperatures decreasing steadily to ~ 21 °C at 200 m. Salinity decreases slightly at 95–100 m (~ 40.35–40.40 PSU) and stabilizes at ~ 40.65 PSU below 130 m.

Within the RCE climax depth range (120–160 m), salinity remains relatively stable at ~ 40.60–40.65 PSU across most casts. In this range, temperature decreases with the depth gradient from 25 to 23 °C during the end of summer and from 23 to 21 °C during early summer.

Chlorophyll-a concentration profiles indicate the presence of a defined DCM between ~ 70 and 110 m in most casts (Fig. S1). During the end of summer (e.g., CHR0043–45, October 2023), Chl-a peaks at ~ 80–100 m, with concentrations approaching 0.2 mg/m^3. In early summer (e.g., CHR0311, NTN0181), the DCM is more pronounced, with elevated Chl-a values observed between 60 and 110 m, with a concentration reaching a peak > 0.8 mg/m^3. Within the RCE climax depth range (120–160 m), Chl-a concentrations remain consistently low (< 0.2 mg/m^3), indicating extremely limited photosynthetic activity.

Comparison of the mesophotic and rariphotic benthic assemblages' composition

Quantitative video analysis showed that the MCE community, between approximately 80 and 103 m depth, was dominated by CCA, followed by zooxanthellate scleractinians

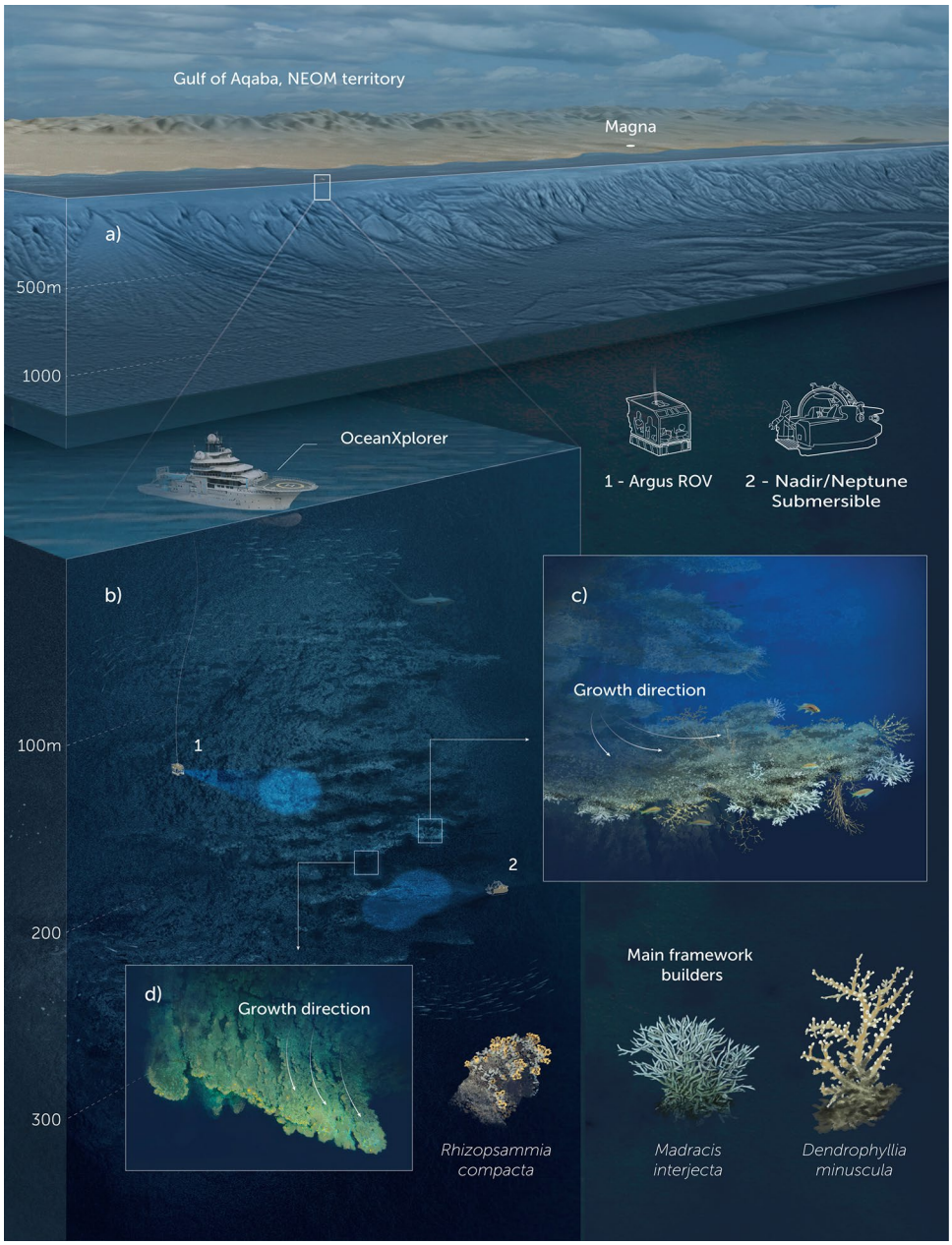

Fig. 6 Overview of the GoA RCE described north of Magna. **a** Continental slope off the city of Magna; **b** exploration assets and bathymetric extension of the RCE, with details of **c** *Madracis interjecta* and *Dendrophyllia minuscula* bioherms, and **d** *Rhizopsammia compacta* bio-stalactites in cavities. Growth direction of the bioherms is indicated by white arrows

and alcyonaceans (Fig. 7a, b; Table S1). Antipatharians and sea whips sensu lato represented a minor component of the benthic community, while a few azooxanthellate scleractinians were present in the lower part of the MCE under small cervices. Large portions of rocky substrate, together with sediment and rubble, were evident. Below the shelf break, approximately 110 m depth, the RCE benthic community was dominated by a bryozoan-foraminifer complex, followed by alcyonaceans, azooxanthellate scleractinians and antipatharians (Fig. 7c, d; Table S1). Sea whips and CCA were rare, the latter present only in the upper part of the RCE, while zooxanthellate scleractinians were absent. Unidentified hard bottom was also present, while mobile sediment was rare compatibly with the moderate to steep inclination of the seafloor typical of the GoA RCE, and differently from the MCE.

Observed anthropogenic impacts

We observed a few abandoned fishing lines, entangled in the coral bioherms (Fig. S4) at all GoA RCE sites, attesting to the occurrence of fishing practices down to more than 200 m depth. Some of the fishing lines had been damaging the frame-building corals. No other signs of stress on the community, nor marine litter, were observed during the ROV and submersible dives.

Table 3 List of fish taxa observed, with the maximum depth recorded in this study and the maximum reported depth from FishBase or relevant literature (a: Baranes & Golani 1993; b: Schuhmacher et al., 1989; c: Moazzam & Osmany 2014; d: Reef Ecology Lab pers. obs.; e: Andradi-Brown, 2019; f: Khalaf et al. 2019). New depth records are in bold, and Red Sea endemic species are indicated with *. Classification within the Red List by the International Union for the Conservation of Nature: least concern (LC); vulnerable (V); endangered (E); not assessed (na)

Class	Family	Species	Maximum depth (m) in this study	Maximum reported depth (m)	IUCN Status
Chondrichthyes	Alopiidae	*Alopias pelagicus Nakamura, 1935*	120	300	E
	Carcharhinidae	*Carcharhinus plumbeus* (Nardo, 1827)	230	500[a]	E
		Sphyrna lewini (Griffith & Smith, 1834)	120	275	
	Torpedinidae	*Torpedo panthera* Olfers, 1831	103	350	E
Osteichthyes	Anomalopidae	*Photoblepharon steinitzi* Abe & Haneda, 1973	137		LC
	Anthiadidae	Anthiadidae sp.	115		
		Plectranthias sp. 1	200		
		Plectranthias sp. 2	152		
		Plectranthias sp. 3	211		
		Pseudanthias gibbosus (Klunzinger, 1884)	161	150	LC
		Pseudanthias* cf. *lunulatus (Kotthaus, 1973)	130	75	
		Pseudanthias heemstrai Schuhmacher, Krupp & Randall, 1989 *	132	67[b]	na
		Pseudanthias taeniatus (Klunzinger, 1884) *	127	40	LC
	Apogonidae	*Ostorhinchus* sp.	140		
	Carangidae	*Seriola rivoliana* Valenciennes, 1833	226	245	LC
	Chaetodontidae	***Chaetodon paucifasciatus*** Ahl, 1923 *	150	65	LC
		Roa jayakari (Norman, 1939)	207	280	LC
	Diodontidae	***Cyclichthys spilostylus*** (Leis & Randall, 1982)	170	110[c]	na
	Holocentridae	*Myripristis chryseres* Jordan & Evermann, 1903	150	350	LC
		Sargocentron ittodai (Jordan & Fowler, 1902)	102	190	LC
	Labridae	***Bodianus opercularis*** (Guichenot, 1847)	168	75	LC
		Cirrhilabrus blatteus Springer & Randall, 1974 *	165	50	LC
		Labridae sp.	180		
		Labroides dimidiatus (Valenciennes, 1839)	170	100	LC
	Lutjanidae	*Lutjanus bohar*	118	180	LC
		Lutjanus kasmira (Forsskål, 1775)	129	265	LC
		Pristipomoides filamentosus (Valenciennes, 1830)	213	400	LC
	Mullidae	*Parupeneus rubescens* (Lacepède, 1801)	148	200[a]	LC
	Muraenidae	*Gymnothorax flavimarginatus* (Rüppell, 1830)	143	150	LC
	Ostraciidae	***Ostracion cyanurus*** Rüppell, 1828	190	30[d]	LC
	Pomacanthidae	***Apolemichthys xanthotis*** (Fraser-Brunner, 1950) *	148	35	LC
		Genicanthus caudovittatus (Günther, 1860)	120	70	LC
	Pomacentridae	*Chromis pelloura* Randall & Allen, 1982 *	206	200[a]	na
	Scorpaenidae	*Pterois miles* (Bennett, 1828)	130	304[e,f]	LC
		Scorpaenidae sp.	125		
	Serranidae	*Cephalopholis sexmaculata* (Rüppell, 1830)	127	150	LC
		Epinephelus fasciatus (Forsskål, 1775)	150	227[f]	LC
		Epinephelus morrhua (Valenciennes, 1833)	211	400[f]	LC
		Liopropoma lunulatum (Guichenot, 1863)	147	350	LC
		Plectropomus marisrubri Randall & Hoese, 1986 *	140	30[d]	V
		Variola louti (Forsskål, 1775)	220	300[f]	LC
	Symphysanodontidae	***Symphysanodon disii*** Khalaf & Krupp 2008 *	200	150	na
	Synodontidae	*Synodus* sp.	150		
	Tetraodontidae	***Arothron hispidus*** (Linnaeus, 1758)	152	50	LC

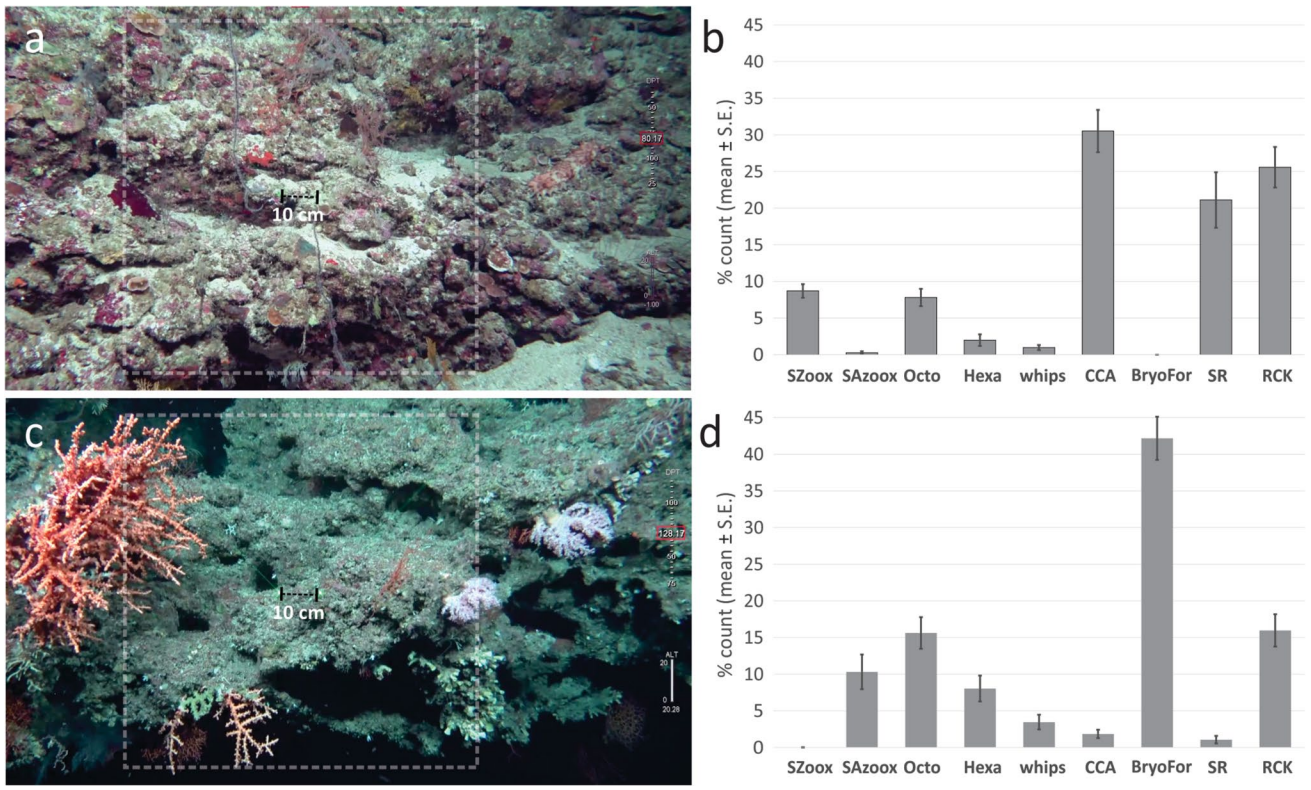

Fig. 7 Characterization of the benthic assemblages composition in the lower mesophotic and rariphotic zones in the Gulf of Aqaba off the Neom coast. **a** Example of the lower MCE; **b** average percentage cover (±standard error) of the examined biotic and abiotic categories in the lower MCE; **c** example of the GoA RCE; **d** Average percentage cover (±standard error) of the examined biotic and abiotic categories in the GoA RCE. For clarity on scale, the 10 cm distance between the two laser points is indicated in panels a and c

Discussion

The pioneering explorations along the Israeli coast of the Gulf of Aqaba by Fricke and colleagues (Fricke 1982, 1996; Fricke and Hottinger 1983) revealed a first insight on the GoA RCE, highlighting the presence of *M. interjecta* bioherms and the minor contribution of *D. minuscula*. Our study provides a detailed description of this peculiar association, reporting the occurrence of extensive formations and different bioherm typologies. We also highlighted the spectacular three-dimensional ecosystem resulting from the combination of the different frame-building corals and the several associated benthic taxa. The ecosystem observed by Fricke (1996, and reference therein), although less structured and diversified than the one here reported, might represent the terminal extension of a discontinuous belt of GoA RCE that, where fully developed, displays all the three bioherm types. Finally, we provide the first quantitative characterization of the GoA RCE benthic assemblage composition and its comparison with the lower MCE in the same zone. In fact, MCEs in the Gulf of Aqaba have been investigated with a focus on the upper mesophotic range off the Israeli coastline (Alamaru et al. 2009; Eyal and Loya 2016; Eyal-Shaham et al. 2016; Eyal et al. 2019a, b; Kramer et al. 2019). Quantitative assessments reached a maximum depth of 60 m (Eyal et al. 2019b) and provided a detailed characterization of the benthic assemblages from the shallow photic to the upper mesophotic zone. There, zooxanthellate corals still occur accounting on average for 20% of the benthic cover and the CCA cover is higher than in the photic zone ranging from 20 to 40%. This study provides the first quantitative characterization of benthic assemblages' composition in two depth ranges deeper than 60 m in the Gulf of Aqaba.

The Gulf of Aqaba rariphotic coral ecosystem

The Red Sea is a marine biodiversity hotspot with high species richness and endemism of the coral reef dwelling fauna in its euphotic zone (Riegl et al. 2012; DiBattista et al 2016a, b). Mesophotic and deep-sea exploration in the basin revealed unique benthic habitats, bioherms, and coral forests (e.g., Qurban et al. 2014; Bracchi et al. 2023) characterized by higher levels of biological diversity than previously expected (Vicario et al. 2024) due to the unique Red Sea environmental conditions (Roder et al. 2013). The GoA RCE represents a further example of the uniqueness of the Red

Sea's coral ecosystems. Unlike their counterparts worldwide, Red Sea corals are adapted to uniquely warm water temperature and high salinity from the shallow to the deep (Roder et al. 2013; Berumen et al. 2019; Chimienti et al. 2022; Nolan et al 2024; Vimercati et al. 2024). For instance, elsewhere in the world, rariphotic corals occur at temperatures cooler than 16 °C and deep-sea corals between 12 and 4 °C (Roberts et al. 2009; Morato et al. 2020), while the Red Sea water temperature stabilizes at 21–22 °C until its deepest point (Roder et al. 2013; Manasrah et al. 2019; Purkis et al. 2022a). However, some populations are not immune to global warming (Eyal et al. 2022).

With 35 azooxanthellate coral taxa censed and up to three different types of bioherms, the GoA RCE is here recognized as a specific type of coral ecosystem, different from any other found outside the Red Sea at any depth. The upper depth boundary of the GoA RCE lies below the recorded occurrence of the Red Sea MCE (Eyal et al. 2019b), and of deepest known Red Sea zooxanthellate mesophotic specialist scleractinian, *L.* cf *striatus*. These corals can reach up to 145 m depth in the Red Sea (Vimercati et al. 2024 and references therein) highlighting the lower limit that MCEs can reach in the basin. These depth limits may vary locally depending on light availability, as shown by chl-a trends and DCM. The latter generally corresponds to the base of the mixed layer and the upper thermocline, coinciding with a transition zone in temperature and salinity gradients, and in the Red Sea can reach 120 m depth (Raitsos et al. 2013). Our results in terms of seasonal peaks and depth distribution are in agreement with the expected Chl-a range along the Red Sea and the Gulf of Aqaba (Labiosa et al. 2003; Raitsos et al. 2013; Kheireddine et al. 2017). Furthermore, the DCM broadly reached to the lower limit of the MCE and the upper limit of the GoA RCE, a few meters shallower than the maximum value reported for the Red Sea. While formal thresholds distinguishing mesophotic from rariphotic zones are difficult to define at large scale, low chlorophyll levels corresponding to the RCE climax depth range (120–160 m) suggest that this depth range lies beyond the lower limit of the productive mesophotic zone and is more consistent with the interpretation of low-light conditions characteristic of RCEs. The shift in benthic community composition between the MCE and the RCE is sharply marked in our study area by the shelf break at 90–110 m followed by a shaded steep, vertical continental slope, where light incidence on the bottom becomes suddenly lower and where the RCE develops. Although scattered crustose coralline algae are still present in the first meters below the top of the GoA RCE, marking the lower horizon of the mesophotic zone, they do not represent a main component of the RCE benthic assemblages. In fact, the GoA RCE is composed of organisms that do not appear to be light dependent. Corals are particularly noticeable during visual surveys and represent the main primary builders, while encrusting bryozoans and foraminifers (absent in the MCE) play an important role in coating, cementing and reinforcing the biogenic structures, being the main taxa in terms of cover percentage. Several factors—including food availability for the corals, substrate orientation related to water-current exposure, and/or a down-slope succession to a substrate type that is less suitable for coral settlement—might limit the 200 m lower depth boundary of the GoA RCE. Below this depth, the GoA RCE benthic assemblages are replaced by what appear like laminar micrite crusts with little structural complexity. Similar structures were already described by Fricke (1996: Fig. 7) along the Israeli coast. Their analysis revealed that the micrite crusts origin depends on a combination of abiotic and biotic processes. The growth rate of this crust is slow (3.5–10 mm per 1000 years) and linked to the activity of small, encrusting serpulids and bryozoans (Brachert and Dullo 1991).

Three bioherm morphologies

Three distinct GoA RCE bioherm types were here identified and described, two of which were previously unknown. The size and structural diversity of the GoA RCE bioherms, fully built by three distinct azooxanthellate and colonial scleractinian species, take us back to the classic question by Schuhmacher and Zibrowius (1985) "*what is hermatypic?*" Following the nomenclature proposed by those authors who also cited the Red Sea case of *M. interjecta* and *D. minuscula* bioherms (Fricke and Hottinger 1983), these two species and *R. compacta* are to be considered azooxanthellate constructional species. Indeed, the constructional role of deep azooxanthellate *Madracis* and Dendrophylliidae species has been long recognized worldwide (Roberts et al. 2009; Cedeño-Posso et al. 2022).

When growing on a steeply inclined surface, the GoA RCE is characterized by the development of unique shelf-like bioherms developing all along its bathymetric range, giving the appearance of an intricate and highly three-dimensional suspended "coral palace." Similar morphologies have been described from the Coral Sea, where mesophotic edges occur between 110 and 130 m depth (Beaman et al. 2016). However, those structures seemed to be mostly created by erosional rather than accretional processes, linked to the Pleistocene sea-level lowstands (Beaman et al. 2016). Differently to the GoA RCE, most of the MCEs known from both the Red Sea (Fricke and Knauer 1986; Eyal et al. 2019a, b) and other tropical areas of the world (Turner et al. 2017; Loya et al. 2019) are typically shaped by zooxanthellate corals that eventually built reef-like ecosystems on flat or sloping seabed. On the contrary, lower MCEs and RCEs are often represented by antipatharian and/or alcyonacean coral forests developing on primarily rocky substrates without a significant contribution by scleractinian corals (Rossi

et al. 2017; Stefanoudis et al. 2019; Chimienti et al. 2020). To the best of our knowledge, *Dendrophyllia cornigera* beds represent the only other RCE built by a scleractinian species. This RCE develops on flat Mediterranean muddy bottoms as an aggregation of different *D. cornigera* colonies (Enrichetti et al. 2023). Other recognized coral ecosystems primarily built by scleractinians develop in aphotic conditions, attaining at the former deep sea. Several examples are known from the Red Sea (Qurban et al. 2014; Nolan et al. 2024), as well as from all the world's oceans (Roberts et al. 2009), where coral mounds or coral framework can be built, displaying a different structure and composition from the GoA RCE.

The discovery of a previously unknown type of columnar bioherm hanging from cavity ceilings and the lower side of shelf-shaped bioherms is also noteworthy because the formations are built by *R. compacta* which, to date, has not been recognized as constructional (Roberts et al. 2009). Thus, its fundamental role as an ecosystem engineer is novel. Described originally from a wreck off the coast of Musandam (Oman) at 30 m depth (Sheppard and Sheppard 1991), the species was subsequently reported from South Africa (Cairns and Keller 1993) and Jordan (Al Tawaha et al. 2019), also from a wreck at 30 m depth. The known colonies are generally small, encrusting with distinct corallites or phaceloid. In the GoA RCE, this species occurs deeper than previously recorded, and grows into metric colonies, the largest ones fusing together and forming bio-stalactites. This suggests that the depth range of *R. compacta* has been underestimated, likely due to an insufficient sampling effort at rariphotic depths, and that the requirements for this species to become constructional are best met in the low-light conditions of a RCE.

Fish fauna

The GoA RCE hosts a rich fish community that is distinct from any previously described Red Sea fish communities. While shallow and upper mesophotic fish communities of the northern Red Sea have been characterized in situ before (Brokovich et al. 2010; Pombo-Ayora et al. 2024), regional records from lower mesophotic and rariphotic depths are based primarily on fished specimens (Baranes and Golani 1993; Khalaf et al. 2019). Our surveys offer one of the first in situ assessments of fish communities inhabiting the lower mesophotic and rariphotic zones of the Red Sea. This is particularly noteworthy because of the high biodiversity and endemism of the Red Sea. Notably, endemism in Red Sea fishes increases with depth: 50% of Red Sea fishes living at depths greater than 200 m are considered endemic (Bogorodsky and Randall 2019).

Rariphotic fish communities are known to be both diverse and distinct from shallower reef fauna (Baldwin et al. 2018). Due to the lack of comparable Red Sea studies at rariphotic depths, it is difficult to ascertain whether the rich and unique fish community of the RCE described in this study is tied to the evidently unique habitat or simply reflects the underexplored nature of these depths. The high structural complexity of the GoA RCE bioherms provides valuable spaces for reef dwelling species. High structural complexity and live coral diversity are known to correlate with increased reef fish abundance and diversity (Gratwicke and Speight 2005; Komyakova et al. 2013). It is therefore likely that the GoA RCE bioherms support a greater fish diversity and abundance compared to the surrounding habitats with lower complexity and benthic diversity. This aligns with unpublished data and personal observations of nearby rariphotic habitats, but additional studies are needed to establish how unique these fish communities are.

The depth range extensions reported in this study further highlight the understudied nature of rariphotic fish communities in the Red Sea. The distinctively warm waters of the Red Sea allow warm-adapted species to inhabit greater depths than recorded elsewhere (Türkay 1996), suggesting that continued exploration could reveal additional depth records for both Red Sea endemics and widespread species. While the GoA RCE appears to act as a potential deep refuge for certain shallow water reef species, such as *Arothron hispidus*, *Chaetodon paucifasciatus*, and *Pseudanthias taeniatus*, the absence of most other shallow water species indicates that it is not a general refuge for shallow reef fish communities. Instead, the GoA RCE hosts a distinct fish community that warrants protection due to its unique species and composition.

Further exploration of RCEs is likely to yield additional new Red Sea records, such as *Sacura boulengeri* (Nunes Peinemann et al. 2022) and *Seriola rivoliana*, as documented in the present study. The discovery of *Seriola rivoliana* is particularly noteworthy, as it highlights the potential for uncovering new records even among highly mobile, large, and conspicuous fishes. Targeted rariphotic collection efforts, especially those focusing on small reef dwelling species, have a high potential to uncover undescribed fish species. It is likely that several species inhabiting the GoA RCE remain undescribed, including some reported here and others that were likely overlooked.

The GoA RCE north of Magna: implications for conservation

The GoA RCE developed at its fullest extent at the site north of Magna city. Here, seabed complexity is promoted by the differential subaerial weathering and collapse of the composite Pleistocene lowstand shoreline, generating ample attractive settlement substrate for a diverse assemblage of calcifying zoobenthos. Locally, the differential bedding of the sandstone was colonized in such a way

that the more prominent the original depositional beds, the more extensive the biogenic overhangs that nucleated from them. In this way, it seems that the extraordinary diversity and degree of bioconstruction in the GoA RCE at the Magna site might, in part, be ascribed to its antecedent topography. The resulting substrate subsequently provided unique edaphic conditions promoting the success of the GoA RCE. The abundance of rheophilic species (e.g., *D. minuscula* and several Antipatharia and Alcyonacea) typically found facing south toward the Tiran Strait (sill at 265 m depth) suggests the presence of currents, possibly driven by the inflow of the north Red Sea water toward the Magna area (Manasrah et al. 2019). Moreover, wind-induced upwelling occurs in the area (Labiosa and Arrigo 2003), and cyclonic and anti-cyclonic eddies are present along the Gulf axis at least in the upper 300 m of the water column (Manasrah et al. 2019). Therefore, the Magna GoA RCE likely benefits from the combination of these hydrodynamic patterns providing food sources and dispersing larvae.

Despite the tolerance of the Red Sea marine biota to warm seawater temperatures, we cannot exclude a potential negative effect of global ocean warming at mesophotic depths, like the one expected for most of the MCEs worldwide (Smith et al. 2019) and already documented on temperate coral ecosystems (Morato et al. 2020). Moreover, local anthropogenic activities such as bottom-contact fishing gear and unregulated coastal development can alarmingly threaten MCEs and RCEs, affecting their ecosystem services. Among these services, the complex three-dimensional structure of the GoA RCE highlights its role in the carbon stock within the Gulf of Aqaba, together with shallower (Heiss 1995) and deeper (Nolan et al. 2024) ecosystems. Given the Saudi Vision 2030 and its focus on sustainable development and biodiversity protection, fundamental knowledge about Red Sea ecosystems of great conservation importance is essential for policy makers to support the ecosystem-based management of human activities. In this framework, the exceptional RCE north of Magna represents an unprecedented biodiversity hotspot and a top priority site for conservation.

Acknowledgements We warmly thank Neom for organising, coordinating, and facilitating the research expeditions in 2020, 2022 and 2023. OceanX, and the Captain and the crew of OceanXplorer are warmly thanked for their operational and logistical support. We would also like to thank Ivan D. Gromicho for the illustration in Fig. 6. G. Chimienti was supported by the Italian Ministry of Education, University and Research (PON 2014–2020, Grant AIM 1807508-1, Linea 1). The material and KAUST team logistics, collected material identification and video analyses were supported by KAUST (award FCC/1/1973-50-01 and baseline research funds to F. Benzoni, and to M.L. Berumen). S. Purkis was funded by NASA ROSES award, MarineVERSE, 20-BIODIV20-0108.

Author contributions Conceptualization: GC, FB; Methodology: GC, FM, FB; Formal analysis and investigation: all authors; Writing—original draft preparation: GC, FB; Writing—review and editing: all authors; Funding acquisition: GC, SJP, MB, AAE, FB; Resources: MB, FB; Supervision: FB.

Funding Open access publishing provided by King Abdullah University of Science and Technology (KAUST).

Data availability Data is provided within the manuscript or supplementary information files. Additional data are availbale from the corresponding authors upon reasonable request.

Declarations

Conflict of interest The authors declare that they have no conflict of interest.

References

Al Tawaha M, Benzoni F, Eid E, Abu Awali A (2019) The hard corals of Jordan, a field guide. The Royal Marine Conservation Society of Jordan, Amman, Jordan, p 432

Alamaru A, Loya Y, Brokovich E, Yam R, Shemesh A (2009) Carbon and nitrogen utilization in two species of Red Sea corals along a depth gradient: insights from stable isotope analysis of total organic material and lipids. Geochim Cosmochim Acta 73:5333–5342

Anderson J, Baranes A, Goren M (2011) Redescription of the perciform fish *Symphysanodon disii* (Symphysanodontidae) from the Gulf of Aqaba, Red Sea, with comments on *S. pitondelafournaisei* and sexual dimorphism in the genus. Zootaxa 3027:1–8. https://doi.org/10.11646/zootaxa.3027.1.1

Andradi-Brown DA (2019) Invasive Lionfish (Pterois volitans and P. miles): distribution, impact, and management. In: Loya Y, Puglise K, Bridge T (eds) Mesophotic coral ecosystems. Coral Reefs of

the World, vol 12. Springer, Cham. https://doi.org/10.1007/978-3-319-92735-0_48
Baldwin CC, Tornabene L, Robertson DR (2018) Below the mesophotic. Sci Rep 8:4920. https://doi.org/10.1038/s41598-018-23067-1
Baranes A, Golani D (1993) An annotated list of deep-sea fishes collected in the northern Red Sea, Gulf of Aqaba. Isr J Ecol Evol 39:299–336. https://doi.org/10.1080/00212210.1993.10688725
Beaman RJ, Bridge TCL, Lüter C, Reitner J, Wörheide G (2016) Spatial patterns in the distribution of benthic assemblages across a large depth gradient in the Coral Sea, Australia. Mar Biodivers 46:795–808. https://doi.org/10.1007/s12526-015-0434-5
Berumen ML, Arrigoni R, Bouwmeester J, Terraneo TI, Benzoni F (2019) Corals of the Red Sea. In: Voolstra CR, Berumen ML (eds) Coral reefs of the Red Sea. Springer, Cham, pp 123–155. https://doi.org/10.1007/978-3-030-05802-9_7
Blyth-Skyrme VJ, Rooney JJ, Parrish FA, Boland RC (2013) Mesophotic coral ecosystems—potential candidates as essential fish habitat and habitat areas of particular concern. Pacific Islands Fishery Science Center, National Marine Fishery Science Center Administrative Report H-13-02, pp 53
Bogorodsky SV, Randall JE (2019) Endemic fishes of the Red Sea. Springer, Cham, pp 239–265
Bracchi VA, Purkis SJ, Marchese F, Nolan MKB, Terraneo TI, Vimercati S et al (2023) Mesophotic foraminiferal-algal nodules play a role in the Red Sea carbonate budget. Commun Earth Environ 4:288. https://doi.org/10.1038/s43247-023-00944-w
Brachert T, Dullo C (1991) Laminar micrite crusts and associated foreslope processes, Red Sea. J Sediment Petrol 61:354–363. https://doi.org/10.1306/D426770D-2B26-11D7-8648000102C1865D
Brokovich E, Ayalon I, Einbinder S, Segev N, Shaked Y, Genin A, Kark S, Kiflawi M (2010) Grazing pressure on coral reefs decreases across a wide depth gradient in the Gulf of Aqaba, Red Sea. Mar Ecol Prog Ser 399:69–80. https://doi.org/10.3354/meps08354
Cairns SD, Keller NB (1993) New taxa and distributional records of azooxanthellate Scleractinia from the tropical south–west Indian Ocean, with comments on their zoogeography and ecology. Ann S Afr Mus 103(5):213–292
Cedeño-Posso C, Vides-Casado M, Rocha V, Borrero-Pérez GH, Polanco FA, Alonso D (2022) Benthic macrohabitat classification and *Madracis* spp. coral patch distribution in a deep-sea marine protected area of Colombia. Front Mar Sci 9:995419. https://doi.org/10.3389/fmars.2022.995419
Chimienti G (2020) Vulnerable forests of the pink sea fan *Eunicella verrucosa* in the Mediterranean Sea. Diversity 12:176. https://doi.org/10.3390/d12050176
Chimienti G, De Padova D, Mossa M, Mastrototaro F (2020) A mesophotic black coral forest in the Adriatic Sea. Sci Rep 10:8504. https://doi.org/10.1038/s41598-020-65266-9
Chimienti G, Terraneo TI, Vicario S, Marchese F, Purkis SJ, Abdulla Eweida A, Rodrigue M, Benzoni F (2022) A new species of *Bathypathes* (Cnidaria, Anthozoa, Antipatharia, Schizopathidae) from the Red Sea and its phylogenetic position. Zookeys 1116:1–22. https://doi.org/10.3897/zookeys.1116.79846
DiBattista JD, Howard Choat J, Gaither MR, Hobbs J-PA, Lozano-Cortés DF, Myers RF et al (2016a) On the origin of endemic species in the Red Sea. J Biogeogr 43:13–30. https://doi.org/10.1111/jbi.12631
DiBattista JD, Roberts MB, Bouwmeester J, Bowen BW, Coker DJ, Lozano-Cortés DF et al (2016b) A review of contemporary patterns of endemism for shallow water reef fauna in the Red Sea. J Biogeogr 43:423–439. https://doi.org/10.1111/jbi.12649
Enrichetti F, Toma M, Bavestrello G, Betti F, Giusti M, Canese S et al (2023) Facies created by the yellow coral *Dendrophyllia cornigera* (Lamarck, 1816): Origin, substrate preferences and habitat complexity. Deep-Sea Res I: Oceanogr Res Pap 195:104000. https://doi.org/10.1016/j.dsr.2023.104000
Eyal G, Cohen I, Eyal-Shaham L, Ben-Zvi O, Tikochinski Y, Loya Y (2019a) Photoacclimation and induction of light-enhanced calcification in the mesophotic coral *Euphyllia paradivisa*. R Soc Open Sci 6:180527. https://doi.org/10.1098/rsos.180527
Eyal G, Tamir R, Kramer N, Eyal-Shaham L, Loya Y (2019b) The Red Sea: Israel. In: Loya Y, Puglise K, Bridge T (eds) Mesophotic coral ecosystems. Coral reefs of the world. Springer, Cham. https://doi.org/10.1007/978-3-319-92735-0_11
Eyal G, Laverick JH, Ben-Zvi O, Brown KT, Kramer N, Tamir R et al (2022) Selective deep water coral bleaching occurs through depth isolation. Sci Total Environ 844:157180. https://doi.org/10.1016/j.scitotenv.2022.157180
Eyal G, Loya Y (2016) Mesophotic reefs examined: Eilat, Red Sea, Israel. In: Baker E, Puglise K, Harris P (eds) Mesophotic coral ecosystems—a lifeboat for Coral reefs? The United Nations Environment Programme and GRID-Arendal, Nairobi/Arendal, pp 28–30
Eyal-Shaham L, Eyal G, Tamir R, Loya Y (2016) Reproduction, abundance and survivorship of two *Alveopora* spp. in the mesophotic reefs of Eilat, Red sea. Sci Rep 6:20964
FAO (2009) International guidelines for the management of deep-sea fisheries in the high seas. FAO, Rome, Italy, pp 73
Fricke H (1982) Lawinen am Meeresgrund. Geo 11:70–76
Fricke H, Hottinger L (1983) Coral bioherms below the euphotic zone in the Red Sea. Mar Ecol Prog Ser 11:113–117
Fricke HW, Knauer B (1986) Diversity and spatial pattern of coral communities in the Red Sea upper twilight zone. Oecologia 71:29–37. https://doi.org/10.1007/BF00377316
Fricke H (1996) Deep-water exploration of the Red Sea by submersible. In: Uiblein F, Ott J, Stachowitsch M (eds) Deep-sea and extreme shallow-water habitats: affinities and adaptations. Biosyst Ecol 11:67–89
Gardiner JS, Waugh P (1939) Madreporaria excluding Flabellidae and Turbinolidae. Scientific reports of the John Murray Expedition, 1933–1934. British Museum (Natural History), London. 6(5):225–242
Gratwicke B, Speight M (2005) Effects of habitat complexity on Caribbean marine fish assemblages. Mar Ecol Prog Ser 292:301–310. https://doi.org/10.1016/j.ecolind.2019.105728
Heiss GA (1995) Carbonate production by scleractinian corals at Aqaba, Gulf of Aqaba, Red Sea. Facies 33:19–34. https://doi.org/10.1007/BF02537443
Kahng SE, Garcia-Sais JR, Spalding HL, Brokovich E, Wagner D, Weil E et al (2010) Community ecology of mesophotic coral reef ecosystems. Coral Reefs 29:255–275. https://doi.org/10.1007/s00338-010-0593-6
Khalaf MA, Krupp F (2008) A new species of the genus *Symphysanodon* (Perciformes: Symphysanodontidae) from the Gulf of Aqaba, Red Sea. Zootaxa 2966:31–36. https://doi.org/10.11646/zootaxa.2966.1.3
Khalaf MA, Maayta SS, Wahsha MA, Manasrah RS, Al-Najjar TH (2019) Community structure of the deep sea fishes in the northern Gulf of Aqaba, Red Sea (Osteichthyes and Chondrichthyes). Zool Middle East 65:40–50. https://doi.org/10.1080/09397140.2018.1552347
Kheireddine M, Ouhssain M, Claustre H, Uitz J, Gentili B, Jones BH (2017) Assessing pigment-based phytoplankton community distributions in the Red Sea. Front Mar Sci 4:132. https://doi.org/10.3389/fmars.2017.00132
Kohler KE, Gill SM (2006) Coral point count with excel extensions (CPCe): A visual basic program for the determination of coral and substrate coverage using random point count methodology. Comput Geosci 32:1259–1269. https://doi.org/10.1016/j.cageo.2005.11.009

Komyakova V, Munday PL, Jones GP (2013) Relative importance of coral cover, habitat complexity and diversity in determining the structure of reef fish communities. PLoS ONE 8:e83178. https://doi.org/10.1371/journal.pone.0083178

Kramer N, Eyal G, Tamir R, Loya Y (2019) Upper mesophotic depths in the coral reefs of Eilat, Red Sea, offer suitable refuge grounds for coral settlement. Sci Rep 9:2663

Labiosa RG, Arrigo KR (2003) The interplay between upwelling and deep convective mixing in determining the seasonal phytoplankton dynamics in the Gulf of Aqaba: evidence from SeaWiFS and MODIS. Limnol Oceanogr 48(6):2355–2368. https://doi.org/10.4319/lo.2003.48.6.2355

Labiosa RG, Arrigo KR, Genin A, Monismith SG, van Dijken G (2003) The interplay between upwelling and deep convective mixing in determining the seasonal phytoplankton dynamics in the Gulf of Aqaba: evidence from SeaWiFS and MODIS. Limnol Oceanogr 48(6):2355–2368

Lesser MP, Slattery M, Leichter JJ (2009) Ecology of mesophotic coral reefs. J Exp Mar Bio Ecol 375:1–8. https://doi.org/10.1016/j.jembe.2009.05.009

Lohrenzen CJ (1966) A method for the continuous measurement of in vivo chlorophyll concentration. Deep-Sea Res 13:223–227

Loya Y, Puglise KA, Bridge T (eds) (2019) Mesophotic coral ecosystems. coral reef of the world 12. Springer International Publishing, AG Cham, Switzerland, p 1003. https://doi.org/10.1007/978-3-319-92735-0

Manasrah R, Abu-Hilal A, Rasheed M (2019) Physical and chemical properties of seawater in the Gulf of Aqaba and Red Sea. In: Rasul NMA, Stewart ICF (eds) Oceanographic and biological aspects of the Red Sea. Springer International Publishing, AG Cham, Switzerland, Springer Oceanography, pp 41–73. https://doi.org/10.1007/978-3-319-99417-8_3

Marenzeller E von (1907) Expedition S. M. Schiff "Pola" in das Rote Meer, nördliche und südliche Hälfte 1895/96–1897/98. Zoologische Ergebnisse 25. Tiefseekorallen. Denkschriften Der Mathematisch-Naturwissenschaftliche Klasse der Kaiserlichen Akademie der Wissenchaften 80:13–25

Marra JF, Lance VP, Vaillancourt RD, Hargreaves BR (2014) Resolving the ocean's euphotic zone. Deep-Sea Res i: Oceanogr Res Pap 83:45–50. https://doi.org/10.1016/j.dsr.2013.09.005

Masetti G, Gallagher B, Calder BR, Zhang C, Wilson M (2017) Sound speed manager: an open-source application to manage sound speed profiles. Int Hydrogr Rev 17:31–40

Moazzam M, Osmany HB (2014) Fishes of family Diodontidae, Ostraciidae and Molidae from Pakistan coast. Int J Biol Biotech 11(4):505–515

Morato T, González-Irusta JM, Dominguez-Carrió C, Wei CL, Davies A, Sweetman AK et al (2020) Climate-induced changes in the suitable habitat of cold-water corals and commercially important deep-sea fishes in the North Atlantic. Glob Change Biol 26:2181–2202. https://doi.org/10.1111/gcb.14996

Nolan MKB, Marchese F, Purkis SJ, Ouhssain M, Kheireddine M, Terraneo TI et al (2024) Habitat suitability models reveal extensive distribution of deep warm-water coral frameworks in the Red Sea. Commun Earth Environ 5:709. https://doi.org/10.1038/s43247-024-01830-9

Nunes Peinemann V, Pombo-Ayora L, Cochran JEM, Marchese F, Chimienti G, Rodrigue M et al (2022) First record of Boulenger's anthias *Sacura boulengeri* (Heemstra 1973) in the Red Sea. J Fish Biol 102(1):294–298. https://doi.org/10.1111/jfb.15254

Pawlik JR, Armstrong RA, Farrington S, Reed J et al (2022) Comparison of recent survey techniques for estimating benthic cover on Caribbean mesophotic reefs. Mar Ecol Prog Ser 686:201–211. https://doi.org/10.3354/meps14018

Pombo-Ayora L, Peinemann VN, Cochran JEM, Eweida AA, Marshall PA, Berumen ML (2024) Diversity, functional redundancy, and vulnerability of reef fish communities of the Saudi Arabian coast, in the northern Red Sea. Reg Stud Mar Sci 78:103798. https://doi.org/10.1016/j.rsma.2024.103798

Purkis SJ, Shernisky H, Swart PK, Sharifi A, Oehlert A, Marchese F et al (2022a) Discovery of the deep-sea NEOM Brine Pools in the Gulf of Aqaba. Red Sea Commun Earth Environ 3:146. https://doi.org/10.1038/s43247-022-00482-x

Purkis SJ, Ward SN, Shernisky H, Chimienti G, Sharifi A, Marchese F, Benzoni F, Rodrigue M, Raymo ME, Abdulla A (2022b) Tsunamigenic potential of an incipient submarine landslide in the Tiran Straits. Geophys Res Lett 49:e2021GL097493. https://doi.org/10.1029/2021GL097493

Qurban MA, Krishnakumar PK, Joydas TV, Manikandan KP, Ashraf TTM, Quadri SI et al (2014) In-situ observation of deep water corals in the northern Red Sea waters of Saudi Arabia. Deep-Sea Res i: Oceanogr Res Pap 89:35–43. https://doi.org/10.1016/j.dsr.2014.04.002

Raitsos DE, Pradhan Y, Brewin RJW, Stenchikov G, Hoteit I (2013) Remote sensing the phytoplankton seasonal succession of the Red Sea. PLoS ONE 8(6):e64909. https://doi.org/10.1371/journal.pone.0064909Riegl

Riegl BM, Bruckner AW, Rowlands GP, Purkis SJ, Renaud P (2012) Red Sea coral reef trajectories over 2 decades suggest increasing community homogenization and decline in coral size. PLoS ONE 7(5):e38396. https://doi.org/10.1371/journal.pone.0038396

Roberts JM, Wheeler A, Freiwald A, Cairns S (2009) Cold-water corals, the biology and geology of deep-sea coral habitats. Cambridge University Press, Cambridge, UK, p 333

Roder C, Berumen ML, Bouwmeester J, Papathanassiou E, Al-Suwailem AM, Voolstra CR (2013) First biological measurements of deep-sea corals from the Red Sea. Sci Rep 3:2802. https://doi.org/10.1038/srep02802

Rosa MR, Alves AC, Medeiros DV, Coni EOC, Ferreira CM, Ferreira BP et al (2016) Mesophotic reef fish assemblages of the remote St. Peter and St. Paul's Archipelago, Mid-Atlantic Ridge. Brazil Coral Reefs 35:113–123. https://doi.org/10.1007/s00338-015-1368-x

Rossi S, Bramanti L, Gori A, Orejas C (eds) (2017) Marine animal forests. The ecology of benthic biodiversity hotspots. Springer International Publishing, AG Cham, Switzerland, pp 1366

Scheer G, Pillai CSG (1983) Report on the stony corals from the Red Sea. Zoologica, Stuttgart 45(133):1–198

Schuhmacher H, Zibrowius H (1985) What is hermatypic? Coral Reefs 4:1–9

Sheppard CRC, Sheppard ALS (1991) Corals and coral communities of Saudi Arabia. Fauna Saudi Arabia 12:1–170

Smith TB, Holstein DM, Ennis RS (2019) Disturbance in mesophotic coral ecosystems and linkages to conservation and management. In: Loya Y, Puglise KA, Bridge T (eds) Mesophotic coral ecosystems. Springer International Publishing, AG Cham, Switzerland, pp 911–929. https://doi.org/10.1007/978-3-319-92735-0_47

Stefanoudis PV, Rivers M, Smith SR, Schneider CW, Wagner D, Ford H et al (2019) Low connectivity between shallow, mesophotic and rariphotic zone benthos. R Soc Open Sci 6:190958. https://doi.org/10.1098/rsos.190958

Tamir R, Eyal G, Kramer N, Laverick JH, Loya Y (2019) Light environment drives the shallow-to-mesophotic coral community transition. Ecosphere 10(9):e02839. https://doi.org/10.1002/ecs2.2839

Terraneo TI, Ouhssain M, Castano CB, Aranda M, Hume BCC, Marchese F et al (2023) From the shallow to the mesophotic: a characterization of Symbiodiniaceae diversity in the Red Sea NEOM region. Front Mar Sci 10:1077805. https://doi.org/10.3389/fmars.2023.1077805

Türkay M (1996) Composition of the deep Red Sea macro- and megabenthic invertebrate fauna. Zoogeographic and ecological implications. In: Uiblein F, Ott J, Stachowitsch M (eds) Deep-sea and extreme shallow-water habitats: affinities and adaptations. Biosyst Ecol 11:43–59

Turner JA, Babcock RC, Hovey R, Kendrick GA (2017) Deep thinking: a systematic review of mesophotic coral ecosystems. ICES J Mar Sci 74(9):2309–2320. https://doi.org/10.1093/icesjms/fsx085

Turner JA, Andradi-Brown DA, Gori A, Bongaerts P, Burdett HL, Ferrier-Pagès C et al (2019) Key questions for research and conservation of mesophotic coral ecosystems and temperate mesophotic ecosystems. In: Loya Y, Puglise KA, Bridge T (eds) Mesophotic coral ecosystems. Springer International Publishing, AG Cham, Switzerland, pp 989–1003. https://doi.org/10.1007/978-3-319-92735-0_52

Vicario S, Terraneo TI, Chimienti G, Maggioni D, Marchese F, Purkis SJ et al (2024) Molecular diversity of black corals from the Saudi Arabian Red Sea: a first assessment. Invertebr Syst 38:IS23041. https://doi.org/10.1071/IS23041

Vimercati S, Terraneo TI, Castano CB, Barreca F, Hume BCC, Marchese F et al (2024) Consistent Symbiodiniaceae community assemblage in a mesophotic-specialist coral along the Saudi Arabian Red Sea. Front Mar Sci 11:1264175. https://doi.org/10.3389/fmars.2024.1264175

Wada H, Suzuki T, Senou H, Motomura H (2020) *Plectranthias ryukyuensis*, a new species of perchlet from the Ryukyu Islands, Japan, with a key to the Japanese species of Plectranthias (Serranidae: Anthiadinae). Ichthyol Res 67:294–307. https://doi.org/10.1007/s10228-019-00725-6